Determination of the effect of pressure on viscosity at high shear rates by using an injection molding machine

VALENTINA VOLPE, ROBERTO PANTANI

Department of Industrial Engineering, University of Salerno, Via Giovanni Paolo II, 132, 84084 Fisciano (SA), ITALY

Correspondence to: Valentina Volpe (E-mail: *vavolpe@unisa.it*)

Keywords

Effect of pressure, injection molding, pressure coefficient, Polystyrene

Abstract The effect of pressure on rheological behaviour of polymer melts is surely a significant phenomenon for polymer processing, and its determination has been the object of several studies which highlighted the difficulties in performing accurate measurements. Even more important is the determination of this effect at very high shear rates, which cannot easily be obtained by conventional rheometers. In this work, a slit rheometer was located at the nozzle of the injection molding machine in order to obtain rheological measurements by means of two pressure transducers. Pressure values were analysed by an original method in order to evaluate the pressure coefficient and the viscosity at zero pressure. The zero pressure viscosity aligned with independent rheological measurements obtained in previous works. The effect of pressure on viscosity was described by means of a parameter whose values resulted to be in line with those obtained in previous works, although the highest shear rates explored in this work were at least one order of magnitude larger.

Introduction

In the last decades, several researchers paid attention to the effect of pressure on the rheological behavior of polymer melts [1-3]. In fact, the pressure levels involved in the transformation processes of polymeric materials can be very high, up to the order of 10^3 bar. Therefore, the conventional assumption that the viscosity of the polymers is constant with pressure, often due to the considerable difficulties in performing accurate measurements of this phenomenon, can lead to an underestimation of the real pressure drops that take place within runners and dies, with consequent difficulties in choosing the correct process variables, or in predicting the material behaviour.

The general pressure dependence of viscosity is usually well described by the Barus equation by means of an exponential function [4]. The coefficient describing the effect of pressure can be at a first approximation considered as a constant, although it is demonstrated [5,6] that it depends on shear rate and temperature. In particular, an increasing of shear rate and temperature generally induces a less pronounced effect of Pressure on viscosity [7]. Direct and indirect methods can be utilized to determine the pressure dependence of viscosity. Cardinaels et al [8] performed direct viscosity measurements under elevated pressures on different polymer melts, using a capillary rheometer equipped with a pressure chamber, in order to present and compare different data analysis schemes to obtain pressure coefficients from high pressure capillary data.

An example of indirect method, based on the principle of free volume to determine the pressure sensitivity of the viscosity was proposed by Utracki and Sedlacek in 2007 [9].

Direct methods to determine the pressure dependence of viscosity can be schematized into two different approaches: the first approach, based on the analysis of non-linearities in the Bagley plots, as proposed by Laun in 1983 [10] or Duvdevani and Klein in 1967 [11], and the second approach,

that requires specific experimental setups, as a multipass rheometer [12] or a counter pressure chamber mounted at the exit of the die of a capillary rheometer [13]. Aho in 2010 [14] determined the pressure coefficient from experimental viscosity data obtained by a capillary rheometer equipped with a downstream pressure chamber. A contribution to the study of the effect of pressure on viscosity comes from Pantani and Sorrentino, who in 2013 [15] utilized both a direct and an indirect method. In particular, they adopted a homemade device to obtain data of viscosity under high pressure together with an indirect method based on the Simha–Somcynsky equation of state, in order to obtain the dependence of free volume on temperature and pressure on the basis of experimental specific volume measurements.

One of the processes in which the effect of pressure on viscosity can be surely significant is injection molding, where pressure levels can be very high. For this process, the study of pressure effect on rheological behaviour of polymer materials becomes interesting when high shear rates are investigated. However, conventional rheometers allow to observe rheological behaviour of polymers only in a limited range of shear rates. In order to overcome this limitation, some devices were developed on purpose. An alternative to the conventional rheometers is to assemble the real process equipment with a die allowing the acquisition of pressure measurements directly during the process [16-18]. Kelly et al. [19] used an instrumented injection molding machine to measure pressure and calculate shear and extensional viscosity at wall shear strain up to 10^7 s^{-1}. In 2011 Aho [20] measured the shear viscosity of PP and PS by means of a slit-die connected to an injection molding machine, obtaining for all materials results comparable with the ones acquired by capillary and rotational rheometers. The effect of pressure on viscosity was not considered in that work. Friesenbichler et al. [21] utilized a standard injection mold with interchangeable dies mounted on a conventional injection molding machine to measure viscosity in time at high shear rate.

In this work, an atactic polystyrene grade commonly used in injection molding process, was adopted to analyze the effect of pressure on viscosity at high shear rates. In particular, a slit rheometer was located at the nozzle of an injection molding machine in order to obtain in-line rheological measurements by means of two pressure transducers. Pressure values were analyzed by an original method to evaluate the pressure coefficient and the viscosity at zero pressure.

Material

A general purpose Polystyrene (PS 678E) supplied by Dow Chemicals, commonly used in injection molding process, was adopted in this work. Polystyrene 678E, whose properties have been well characterized in literature [22-25], has a molecular weight distribution characterized by Mn=(87±4) 10^3, Mw=(250±20) 10^3 and Mz=(490±60) 10^3.

The mathematical description of the viscosity is essential for modeling and simulation in polymer processes. In order to describe the shear thinning behavior of a polymer melt over a large range of shear velocity, a Cross Model can be adopted:

$$\eta(\mathrm{T},\mathrm{P},\dot{\gamma}) = \frac{\eta_{\mathrm{N}}(\mathrm{T},\mathrm{P})}{1+\left(\frac{\eta_{\mathrm{N}}(\mathrm{T},\mathrm{P})\dot{\gamma}}{\tau^*}\right)^{1-\mathrm{p}}} \quad (1)$$

where η_N, is the viscosity at zero shear rate, $\dot{\gamma}$ is the shear rate, τ^* is the characteristic shear stress (where there is the change between Newtonian and shear thinning behavior) and p is the flow index. In the above equation, the Newtonian shear viscosity, η_N, can be assumed to be a function of Temperature T and Pressure P according to the following Vogel equation [5]:

$$\eta_N(T,P) = \eta^* e^{\frac{A+kP}{T-T_{ref}}} \quad (2)$$

in which η^*, k and T_{ref} are constants. Experimental data obtained from independent rheological measurements carried by means of rotational and capillary rheometers on the same material adopted in this work [5,7] allowed to determine the parameters of equations 1 and 2 reported in Table 1. These parameters were used as a reference for this work.

TABLE 1 Parameters of Cross–Vogel equation for aPS 678E [7].

η* [Pa*s]	0.63
A [°C]	1348
T_{ref} [°C]	50.9
p [-]	0.17
τ* [Pa]	35201
k [°C/Pa]	1.00E-05

Injection Molding machine

A 70-ton Negri-Bossi reciprocating screw injection molding machine was used for the experiments. The screw diameter was 25 mm. A slit rheometer was located at the nozzle of the machine and allowed obtaining in-line rheological measurements by means of two pressure transducers, which can measure the pressure in a range from 0 to 2000 bars (Figure 1). These pressure transducers are housed along the flow direction, at a distance equal to 15 mm and 60 mm from the inlet of the slit. Furthermore, two thermocouples, placed at the inlet and exit of the slit, allowed to measure and control the temperature inside the slit. Differently from the capillary rheometer, that needs a

Bagley correction, a slit rheometer allows obtaining a direct measure of the pressure drop and thus of the viscosity. Obviously, the shear rates that can be attained in the slit depend on the flow rate and on the geometry of the slit. In this work, the flow rate was imposed by the injection molding machine, and two different geometries were chosen for the slits, as reported in Tab. 2.

TABLE 2 Geometry of the slits.

Slit dimensions	**S1**	**S2**
Total Length	120 mm	120 mm
Width	10 mm	20 mm
Thickness (2B)	0.75 mm	2 mm

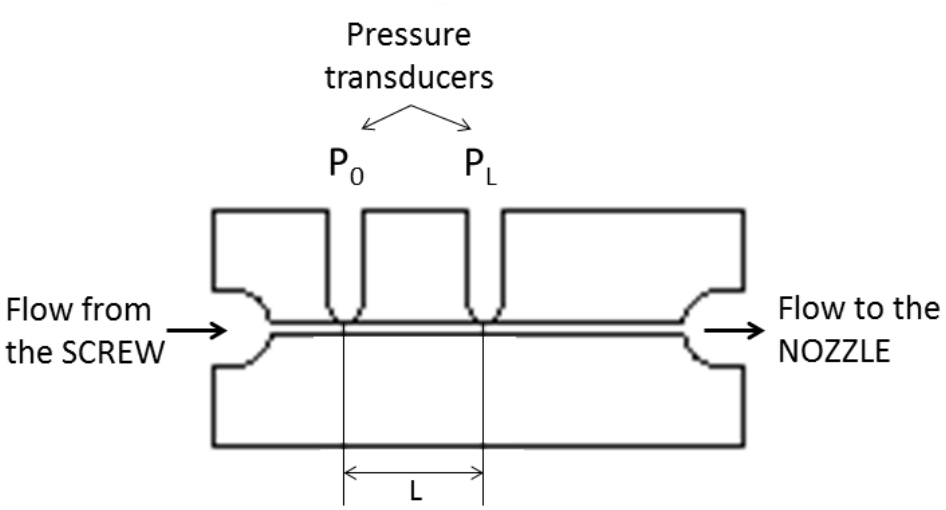

FIGURE 1 Slit rheometer

Experiments were conducted at three injection temperatures (220°C, 240°C and 260°C) and increasing injection flow rates.

A data acquisition system allowed to measure the pressure at the two transducers positions (P_0 and P_L), and the position of the screw during the injection phase. From the screw position, it was

possible to calculate the screw velocity, namely the slope of the curve that represents the screw position versus time during the injection phase and thus imposed flow rate, as the product between the screw velocity and its section. In Figure 2a, we report the pressure profiles acquired by the two transducers when the slit S1 was mounted at the highest and the lowest imposed flow rates adopted in this work (4 cm^3/s and 74 cm^3/s). Figure 2b shows the screw position during injection phase at all different imposed flow rates adopted. As clear from the graphs, the screw position is linearly depending on time and thus the velocity is constant during each test.

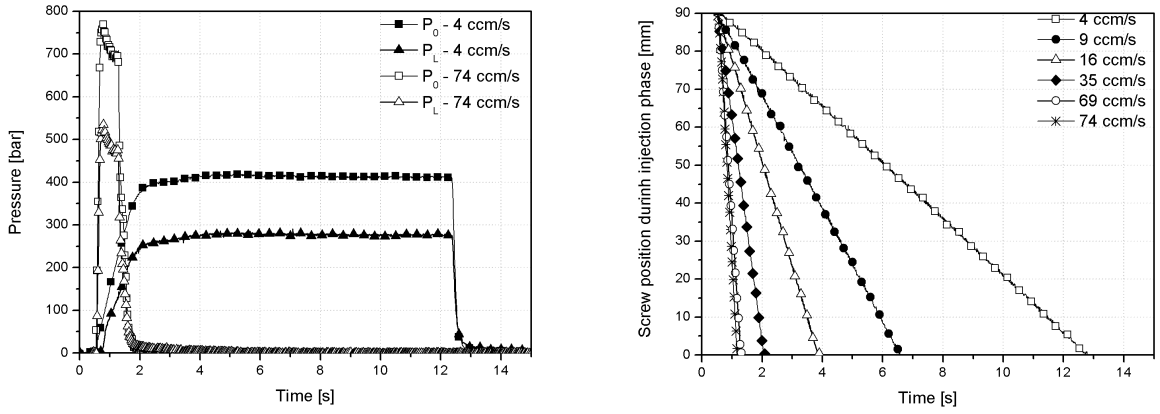

a) b)

FIGURE 2 a) Pressure profiles during injection phase at 4 cm^3/s and 74 cm^3/s; b) Screw position during injection phase at different injection flow rates; thinner slit (S1), injection temperature 240 °C

The pressure plots reported in Figure 2a show that pressure increases from the initial zero value when the melt reaches the transducer position. Then the value keeps on increasing because the flow lenght downwards increases. When the melt reaches the nozzle (which is open to atmosphere) the pressure reaches a maximum value, which is kept until the screw stops.

High pressure viscosity

The flow established within the slit can be analyzed by the equations of motion in rectangular coordinates, with the simplifying assumptions of incompressible fluid, stationary flow and negligible edge effects. The incompressibility is justified by the fact that, according to PVT data [7], at 240°C the specific volume undergoes a 5% change when pressure increases from 0 to 500 bar.

By supposing that the flow takes place predominantly in the flow direction, i.e. along the axis of the slit, and that *B* is the half thickness of the slit, the average velocity *V* can be calculated as the ratio between the imposed flow rate Q_{slit} and the slit section S_{slit}:

$$V = Q_{slit}/S_{slit} \quad (3)$$

$$S_{slit} = W * 2B \quad (4)$$

The shear rate and the viscosity can be related by a power-law:

$$\eta = m\dot{\gamma}^{n-1} \quad (5)$$

where *n* is the flow index and *m* is the consistency index,

The effect of viscous dissipation can be estimated by the Nahme–Griffith number (*Na*), which represents the ratio between the viscous heating and the thermal conduction when the temperature difference is sufficiently large to induce a change in viscosity (equation 3):

$$Na \equiv \frac{V^2 \alpha_\eta \bar{\eta}}{k_T} \quad (6)$$

where V is the average velocity, k_T is the thermal conductivity, $\bar{\eta}$ is a reference viscosity (i.e. the viscosity at the apparent shear rate $\dot{\gamma}_a = 3V/B$), and α_η is the temperature coefficient of viscosity, namely:

$$\alpha_\eta = \left[1 + p\left(\frac{\eta_N \dot{\gamma}_a}{\tau^*}\right)^{1-p}\right] \Big/ \left[1 + \left(\frac{\eta_N \dot{\gamma}_a}{\tau^*}\right)^{1-p}\right] \cdot \frac{A}{\left(T - T_{ref}\right)^2} \tag{7}$$

if eq. 2 is adopted [5]. In the range of shear rates explored in this work, α_η is about 10^{-2} K^{-1} for the adopted PS.

For Nahme–Griffith numbers significantly larger than one, the effect of viscous dissipation considerably changes the viscosity. In the following, the results of the tests with Nahme–Griffith numbers larger than one (which are found here for flow rate higher than 35 cm^3/s for the thinner slit, S1, and higher than 69 cm^3/s for the thicker slit, S2) are represented with a different color.

The viscosity can be evaluated from measurements of pressure drops and flow rates, as:

$$\eta = \frac{\tau_w}{\dot{\gamma}_w} \tag{8}$$

where

$$\dot{\gamma}_w = \dot{\gamma}_a \left(\frac{1+2n}{3n}\right) \tag{9}$$

$$\tau_w = B \frac{\Delta P}{L} \tag{10}$$

and $\Delta P = (P_0 - P_L)$ is the difference in the pressure values measured by the transducers separated by a distance equal to L.

The value of n can be obtained as:

$$n = \frac{\partial \ln\left(-\frac{\Delta P}{L}\right)}{\partial \ln(\dot{\gamma}_a)} \tag{11}$$

In order to evaluate the viscosity at highest pressures reached by the system, the pressures corresponding to the plateau at the end of the injection phase was utilized (Figure 3). In this way, each test allows to measure the viscosity at a certain pressure P_M corresponding to the arithmetic average between the two values provided by the transducers.

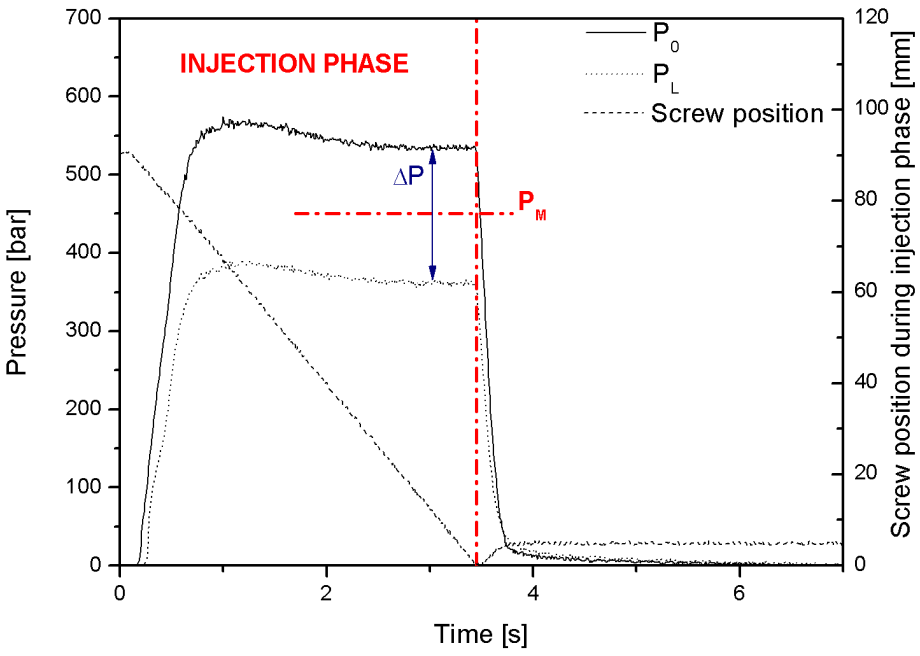

FIGURE 3 Pressure profiles and screw position during injection phase at 16 cm^3/s; thinner slit, injection temperature 240 °C.

Figure 4 shows the results obtained for some of the tests following the method described above. The levels of pressures reached are grouped and reported as an indication close to the points. As a reference, the results of the Cross-Vogel Model (with the parameters reported in table 1) are also reported. The system adopted in this work allows to obtain rheological data up to more than 10^5 s^{-1}, namely close to the limit of capillary rheometers, without the need of a Bagley correction.

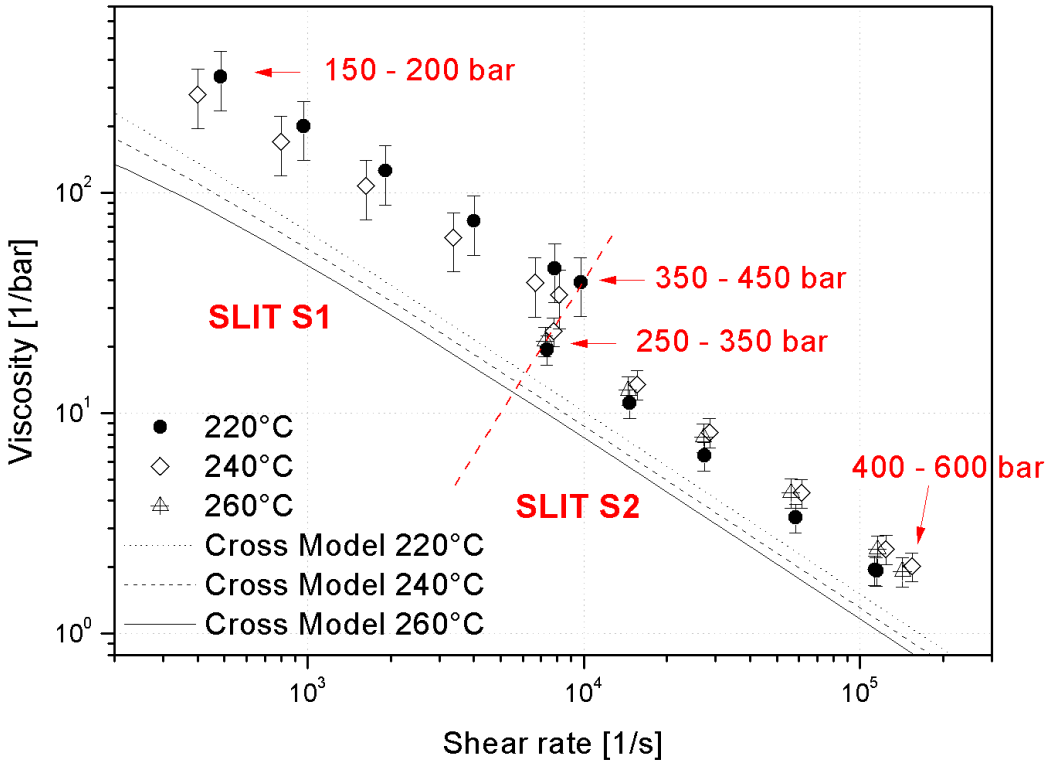

FIGURE 4 Comparison of experimental data of high pressure viscosity at different temperatures with the Cross-Vogel Model prediction at zero pressure. The dotted line separates the data obtained by the two slits. For some of the data, pressures are indicated (refer to table 3 for all the results).

The data of high pressure viscosity are positioned well above the lines that describe independent rheological measurements obtained by the Model at all the three temperatures and zero pressure, and allow to get an idea of the magnitude of the pressure effect on the viscosity measurements. Table 3 reports the values of viscosity at high pressure $\eta(P_M)$ and the average pressures (P_M) for both the two slit geometries and at all the imposed flow rates.

TABLE 3 Viscosity at zero pressure, viscosity at high pressure and average pressures for both the two slit geometers.

	220 °C			**240 °C**			**260°C**		
	η (P=0) [Pa*s]	***P_M [bar]***	***η (P_M) [Pa*s]***	***η (P=0) [Pa*s]***	***P_M [bar]***	***η (P_M) [Pa*s]***	***η (P=0) [Pa*s]***	***P_M [bar]***	***η (P_M) [Pa*s]***
S2 - 4 cm³/s	1.11E+02	221	3.35E+02	7.50E+01	165	2.79E+02	-	-	-
S2 - 9 cm³/s	7.39E+01	257	1.99E+02	4.92E+01	195	1.70E+02	-	-	-
S2 - 16 cm³/s	4.43E+01	301	1.26E+02	4.05E+01	244	1.08E+02	-	-	-
S2 - 35 cm³/s	2.74E+01	360	7.44E+01	2.33E+01	291	6.24E+01	-	-	-
S2 - 69 cm³/s	1.55E+01	417	4.51E+01	1.51E+01	338	3.89E+01	-	-	-
S2 - 74 cm³/s	1.54E+01	441	3.91E+01	1.39E+01	358	3.44E+01	-	-	-
S1 - 4 cm³/s	8.03E+00	252	1.94E+01	1.04E+01	345	2.35E+01	9.54E+00	290	2.12E+01
S1 - 9 cm³/s	5.52E+00	292	1.11E+01	5.87E+00	403	1.35E+01	4.88E+00	350	1.27E+01
S1 - 16 cm³/s	3.09E+00	320	6.40E+00	3.88E+00	450	8.18E+00	3.17E+00	406	7.78E+00
S1 - 35 cm³/s	1.74E+00	366	3.36E+00	2.15E+00	517	4.34E+00	1.89E+00	474	4.35E+00
S1 - 69 cm³/s	1.04E+00	407	1.95E+00	1.27E+00	583	2.42E+00	1.22E+00	540	2.41E+00
S1 - 74 cm³/s	1.20E+00	401	1.93E+00	1.12E+00	603	2.02E+00	-	483	1.91E+00

Quantification of the effect of pressure on viscosity

The consistency index in eq. 5 can be considered to be a function of pressure according to the Barus equation

$$\mathrm{m} = \mathrm{m}_0 \mathrm{e}^{\beta \mathrm{P}} \tag{12}$$

In which β is the parameter which accounts of the effect of pressure on viscosity. It can be considered constant at each shear rate [7]. The pressure gradient along the flow direction can be thus expressed as:

$$-\frac{dP}{dx} = C_1 m_0 e^{\beta P} \tag{13}$$

$$C_1 = \left(V \frac{2n+1}{n}\right)^n \frac{1}{B^{n+1}} \tag{14}$$

where C_1 is a parameter which collects some variables in order to increase the readability of the following equations.

This is the conventional result for the flow of a power law fluid in a slit. Equation 13 can be integrated in the space *L* between two transducers, i.e. between the pressure at the first transducer, P_0, and at the second transducer, P_L

$$\frac{1}{\beta}\left(\mathrm{e}^{-\beta \mathrm{P_L}} - \mathrm{e}^{-\beta \mathrm{P_0}}\right) = \mathrm{C_1 m_0 L} \tag{15}$$

In order to analyze the data collected in this work and to quantify the effect of pressure on viscosity, we propose a simplification of equation 15. In particular, the exponential terms is approximated by a second order polynomial

$$\frac{1}{\beta}\left[\frac{(\beta P_L)^2}{2}-\beta P_L-\frac{(\beta P_0)^2}{2}+\beta P_0\right]=C_1 m_0 L \quad (16)$$

After rearranging one obtains:

$$\frac{1}{\Delta P}=\frac{1}{C_1 m_0 L}-\frac{\beta}{C_1 m_0 L}P_M \quad (17)$$

Where P_M is the average pressure $(P_0+P_L)/2$. According to equation 17, the reciprocal of the pressure difference measured by the two pressure transducers during a test carried out at constant flow rate, should be linearly dependent on the average pressure. Indeed, as shown in figure 2a and 3, since the pressure levels at the transducers increase with time , this causes an increase with time of the average pressure P_M.

Figure 5 shows the reciprocal of the pressure difference obtained from the two pressure transducers during the injection phase ($1/\Delta P$) vs the average pressure, for two different applied injection flow rates. Each plot refers to one injection test.

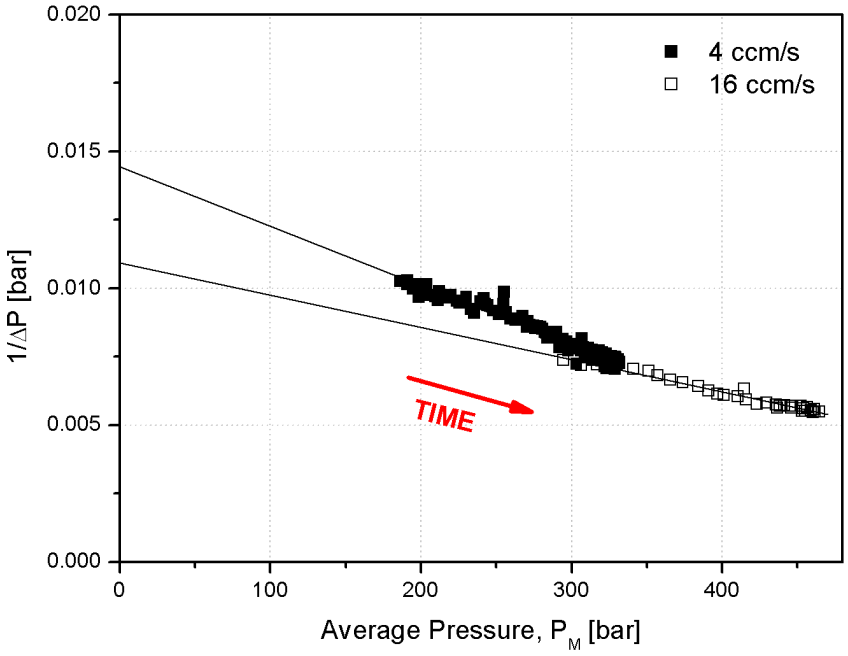

FIGURE 5 Experimental data of *1/ΔP* vs average pressures obtained at 240 °C with the thinner slit S1 at different injection flow rates. The slopes of the lines are proportional to the value of the pressure coefficient at each shear rate.

It is clear that the plots are nearly linear, confirming the analysis carried out in equations 15-17.

The pressure coefficient β can be calculated from the ratio between slope and intercept of the straight lines that best fit the data (Figure 5). For both the slits and at all the injection temperatures, the values of β calculated in this way were plotted vs the corresponding shear rate in Figure 6 and compared with literature results collected on the same material by adopting a capillary rheometer[7].

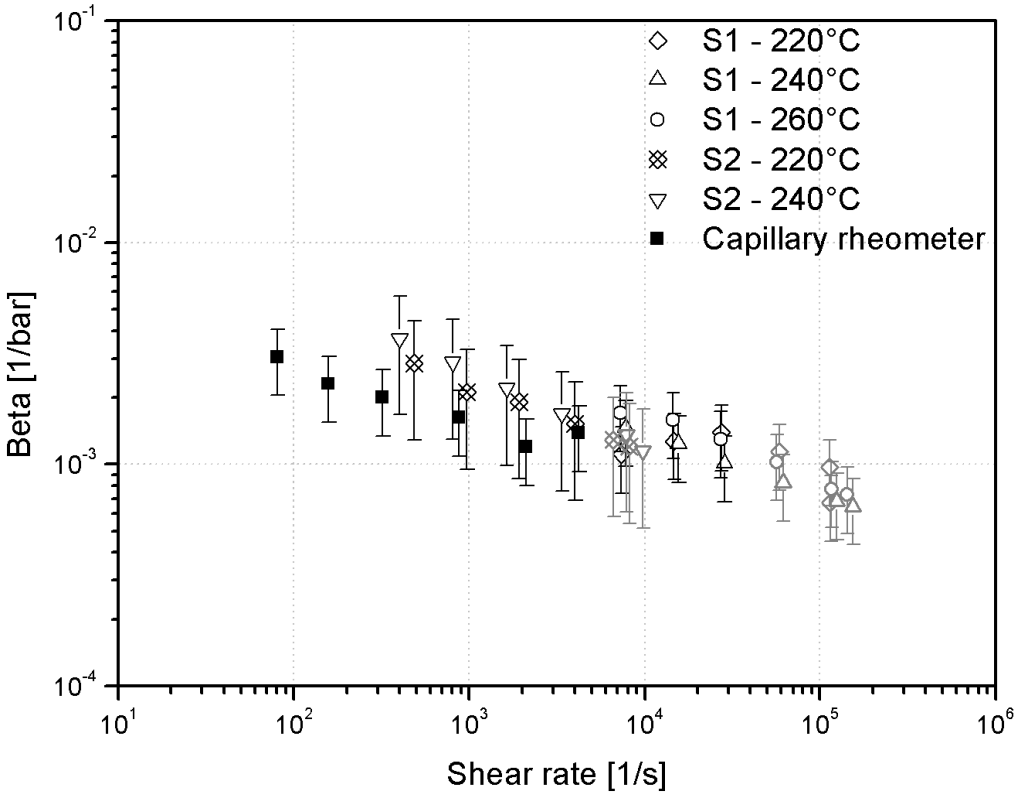

FIGURE 6 Experimental measurements of beta obtained as slope of plots reporting *1/ΔP* vs P_{av}. *"Capillary rheometer"* data series refers to previously obtained data (Pantani and Sorrentino 2009) by adopting a different method. The points in gray represent data with *Na > 1*.

From Figure 6 it is possible to observe that the experimental data obtained with the slit rheometer align with those obtained by the capillary rheometer and extend the data previously collected in a range of shear rate at least one order of magnitude larger. In Figure 6 we also report data which presented Na > 1 (in gray). Considering that the effect of pressure and the effect of temperature on viscosity counteract each other, it should be considered that gray symbols which neglect viscous dissipation should be corrected toward higher values. An estimation of the error made neglecting the dissipative heating can be found in the literature [5]:

$$\frac{\beta_{corr}-\beta}{\beta} = \frac{\alpha_\eta}{\beta}\frac{1}{\rho C_p} \quad (18)$$

where β_{corr} is the corrected value for β assuming adiabatic conditions. For the material adopted in this work $\rho C_p \cong 20\ bar/K$ and thus the correction can be as high as about 50%.

Zero pressure viscosity

The intercepts of the linear plots reported in Figure 5 refer to the values of pressure drops when the average pressure is zero. These values allow to calculate the parameter m_0 and thus to evaluate the viscosity at zero pressure. Figure 7 shows the zero pressure viscosity at different shear rates compared to the Cross-Vogel Model, whose parameters reported in Table 1 were determined by independent rheological measurements [7].

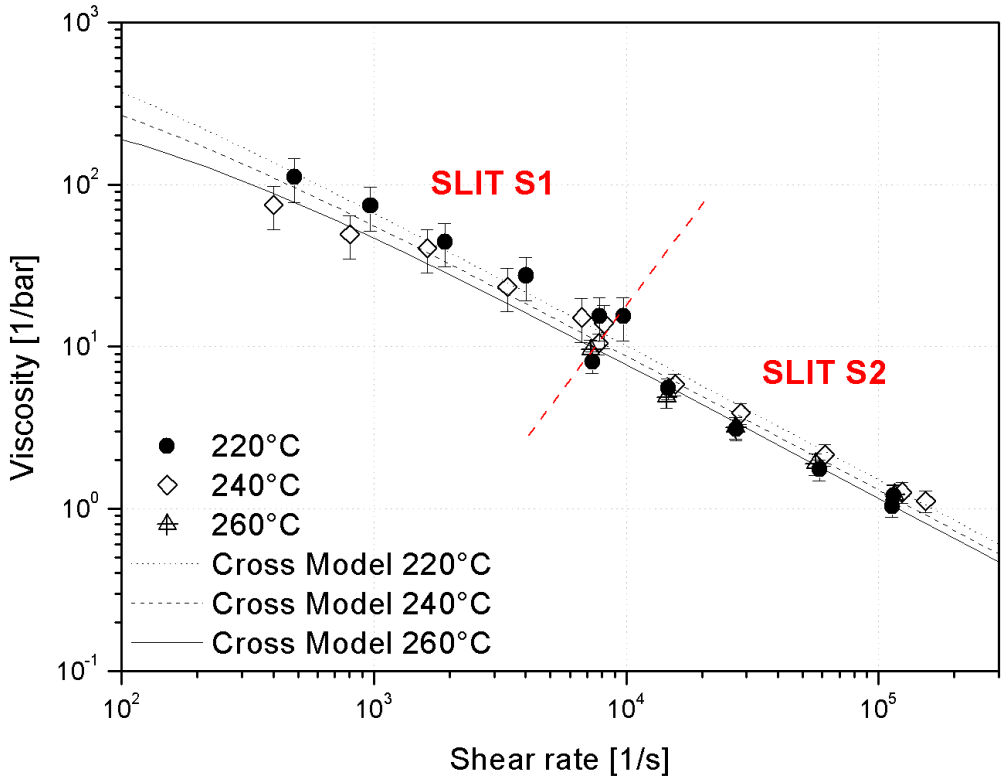

FIGURE 7 Comparison of experimental data of zero pressure viscosity with the Cross-Vogel Model at different temperatures. The dotted line separates the data obtained by the two slits.

The data of zero pressure viscosity are very close to the lines obtained by the model at all the three temperatures. A difference between the measurements made at about te same shear rates by using the two slits persists. The reasons should be explored and could be due to the difficulties in taking measurements at the highest applied flow rates. The differences between the data obtained by the two slits are however of the order of the common data scattering of rheological measurements at high shear rates.

Description of the effect of pressure by Cross-Vogel Model

In order to describe the effect of pressure on viscosity by Cross-Vogel Model, the results of pressure coefficients reported in Figure 6 were utilized to determine the parameter *k* in the Cross-Vogel Model. In particular, the pressure coefficient at constant shear rate can be related to the parameters of the Cross–Vogel Model by the following equations [5]:

$$\beta = \frac{1}{\eta}\left(\frac{\partial \eta}{\partial \mathrm{P}}\right)_{\mathrm{T},\dot{\gamma}} = \frac{1}{\eta}\frac{\partial \eta}{\partial \eta_{\mathrm{N}}}\frac{\partial \eta_{\mathrm{N}}}{\partial \mathrm{P}} \tag{19}$$

$$\beta = \frac{1+p\left(\frac{\eta_N \dot{\gamma}}{\tau^*}\right)^{1-p}}{1+\left(\frac{\eta_N \dot{\gamma}}{\tau^*}\right)^{1-p}}\frac{k}{T-T_{ref}} \tag{20}$$

Assuming the validity of all the other parameters reported in Table 1 (which are consistent with rheological values obtained in this work), the effect of pressure is fully described when the

parameter k is found. In Figure 8 the data of pressure coefficients at the corresponding shear rates were described by the Cross–Vogel equation for different values of the parameter k: from 10^{-5} °C/Pa (namely the original value found by Pantani and Sorrentino) to 1.5 10^{-5} °C/Pa. The values of k which allows to better fit the results obtained in this work also at high shear rates are in the range from 1.3 to 1.5 10^{-5} °C/Pa. These values are higher than the value that allows to well describe the results obtained by capillary rheometer (10^{-5} Pa^{-1}), but still consistent with all the data set, considering the uncertainty of each experimental result.

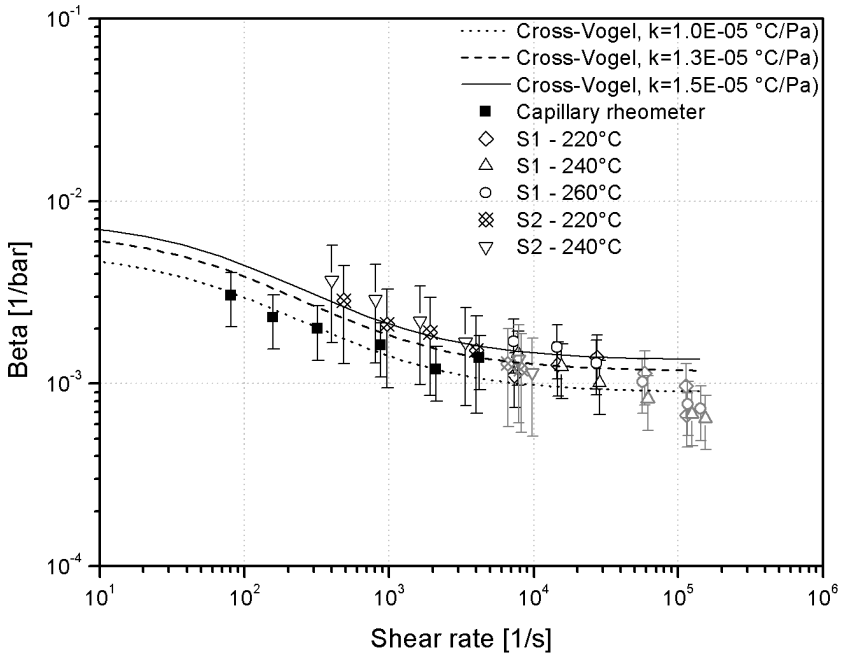

FIGURE 8 Comparison between experimental measurements of beta and the description by Cross–Vogel equation (eq.20).

Conclusions

In this work, the effect of pressure on the viscosity of an atactic polystyrene was studied by using a slit rheometer connected in line with an injection molding machine. The collected data allowed to

assess the viscosity at pressure in the range 150 - 600 bar and shear rates in the range 10^2 - 10^5 s^{-1}. The effect of pressure on viscosity was described by introducing an original analysis of data. The analysis allowed to determine the viscosity at zero pressure and the effect of pressure on viscosity from the time evaluation of pressures measured inside the slit. Both zero pressure viscosity and the parameter describing the effect of pressure resulted to be in line with those obtained in previous works, although the highest shear rates explored in this work were at least one order of magnitude larger. This confirms the validity of the method adopted in this work and widens the knowledge of the rheological behaviour of the adopted material toward shear rates of interest for injection molding.

References

1. Couch, M. A.; Binding, D. M., Polymer 41, 6323 2000.
2. Goubert A, V. J., Moldenaers P, Göttfert A, Ernst B, Appl. Rheol. 11, 26 2001.
3. Kadijk, S. E.; Vandenbrule, B. H. A. A., Polym Eng Sci 34, 1535 1994.
4. Barus, C., Proceedings of the American Academy of Arts and Sciences 27, 13 1891.
5. Pantani, R.; Sorrentino, A., Polym Bull 54, 365 2005.
6. Rodriguez, E.; Fernandez, M.; Munoz, M. E.; Santamaria, A., J Rheol 60, 1199 2016.
7. Sorrentino, A.; Pantani, R., Rheol Acta 48, 467 2009.
8. Cardinaels, R.; Van Puyvelde, P.; Moldenaers, P., Rheol Acta 46, 495 2007.
9. Utracki, L. A.; Sedlacek, T., Rheol Acta 46, 479 2007.
10. Laun, H., Rheol. Acta 22, 171 1983.
11. Duvdevani IJ, K. I., Soc. Pet. Eng. J. 23, 41 1967.
12. Mackley, M. R.; Spitteler, P. H. J., Rheol Acta 35, 202 1996.
13. Li, C.; Jiang, F.; Wu, L. H.; Yuan, X. Y.; Li, X., J Macromol Sci B 54, 1029 2015.
14. Aho, J.; Syrjala, S., J Appl Polym Sci 117, 1076 2010.
15. Sorrentino, A.; Pantani, R., Polym Bull 70, 2005 2013.
16. Bariani, P. F.; Salvador, M.; Lucchetta, G., J Mater Process Tech 191, 119 2007.
17. Claveria, I.; Javierre, C.; Ponz, L., J Mater Process Tech 162, 477 2005.
18. Fernandez, A.; Muniesa, M.; Javierre, C., Polym Test 33, 107 2014.
19. Kelly, A. L.; Gough, T.; Whiteside, B. R.; Coates, P. D., J Appl Polym Sci 114, 864 2009.
20. Aho, J.; Syrjala, S., Polym Test 30, 595 2011.
21. Friesenbichler, W.; Duretek, I.; Rajganesh, J.; Kumar, S. R., Polimery-W 56, 58 2011.
22. Flaman, A. A. M., Plastics in the Environment : Yesterday, Today & Tomorrow, 365 1990.
23. Laven, J., Nonisothermal Capdby Flow of Plastics, Ph.D thesis. Delft. University, Netherlands , 1985.
24. Pantani, R.; Speranza, V.; Titomanlio, G., Polym Eng Sci 41, 2022 2001.

25. Pantani, R.; Titomanlio, G., Int Polym Proc 14, 183 1999.